General comments:

This paper presents receiver-function results from a deployment of OBS instruments in the Celebes Sea. The experiment encountered serious difficulties, with only nine stations usable for this analysis out of twenty-seven deployed. Add to this the difficulties of receiver-function analysis under typical OBS constraints (high noise level and short deployment time), and the authors have done a truly remarkable job getting the most out of this challenging data set. The main results, a Moho step near the Palu-Koro Fault and a low-velocity upper crust near the fault trace, are interesting and look to be robust (the Moho depths match very well between methods, for instance), and the authors sensibly don't place too much weight on less robust results, like the Vp/Vs values retrieved from H-k stacking. As noted below, the writeup is a bit brief and could stand to be clearer about some methodological aspects; I would consider this a minor revision.

(Note that I have deliberately not looked at other comments on this manuscript before writing this; it's best for reviews to be independent.)

Specific comments:

1. Some details on the OBS processing are missing. For instance, did the OBSes have hydrophones? If so, were they used to correct the seismic data in any way?

Reply: Thank you for your comment. The preprocessing workflow of passive-source OBS data follows Yang et al. (2023) and has been described in detail in Text S1 and Text S2 of the supplementary file. The corresponding supplementary description has been added in the revised manuscript at Lines 90–100. We include the preprocessing steps our supplementary material, such as the azimuth correction and the time correction. Regarding the compliance noise correction using the hydrophone data, we did not do it since the hydrophone we used in this experiment are 20 – 100Hz , the low frequency response of the hydrophone is not low enough to remove the pressure noise from the vertical channels. As the low frequency hydrophone or pressure gauge gradually become a 'standard' OBS component nowadays. The hydrophone of the OBSs made by CAS are upgraded this year, so removing compliance noise becomes feasible in future.

Clock drift correction: We observer up to several seconds per year from different OBS in our dataset and the cross-correlation approach provides a robust solution. We estimates and corrects clock errors in both land stations and OBS by leveraging ambient seismic noise cross-correlations across multiple components of motion follow the method by Hable et al. 2018 . Because noise-derived correlations should ideally be symmetric in causal vs. acausal parts, any systematic asymmetry is interpreted largely as a relative time offset (clock error) between the stations. The end result has errors of 0.5 ms with a linear drift assumption, and we applied the corrections linearly over the deployment period. Besides the quartz clock drift without GNSS, the OBS also employ several internal correction which are applied

automatically when exporting the data.

Azimuth correction: The azimuthal corrections of the horizontal components were performed following Niu and Li (2011). The coordinate system from the source to the OBS and the propagation (particle motion) direction of the P wave. A rotation step of 0.1° was applied to rotate the N–E coordinate system into the R–T coordinate system. We employed an SNR-weighted multi-event method to perform a grid search for the optimal back-azimuth angle $\boldsymbol{\theta_a}$. At each grid point, the P-wave transverse component energy was calculated as $\boldsymbol{E_T(\theta_a)}$.

2. For the receiver function deconvolution, what time-domain method was used? From context I would guess the iterdecon technique, but it's not stated explicitly.

Reply: Thank you for your comment. In this study, radial receiver functions were derived for the teleseismic P-wave arrivals using the time-domain iterative deconvolution technique of Ligorría and Ammon (1999). This information has been added in the revised manuscript at Lines 137–139.

3. In figure 3: what order are the RFs presented in? Chronological, or by epicentral distance, or something else? Also, it would be helpful to see an overlay of the expected arrival times for the best-fit H and k, to see what arrivals are being used.

Reply: Thank you for your comment. In Fig. 3, the receiver functions are presented in chronological order of the events. The H–κ stacking procedure automatically searches for the best-fit crustal thickness (H) and Vp/Vs ratio (κ), and therefore the specific phase arrivals used are not explicitly picked. As such, it is not straightforward to overlay individual predicted arrival times on each trace. Instead, the stacking process inherently accounts for the relevant converted phases and multiples to determine the optimal solution.

4. The text on page 7 refers to an anticorrelation between H and surface topography, but this isn't shown directly. A plot might make this more convincing (free-air gravity could also optionally be included). Figure 6 does show this, but doesn't include all stations.

Reply: Thank you for your comment. In the revised manuscript, the anticorrelation between topography and Moho depth is shown in Fig. 6c, where the red dashed line indicates the Moho depth beneath the seafloor topography in the upper panel. In addition, we have added a gravity anomaly profile in the supplementary file (Fig. S16) as supporting evidence for this result.

5. I assume that the traces were stacked before the RF waveform inversion, since a fit to only one trace is shown, but this isn't stated explicitly. Also, was a moveout applied before stacking? And in the inversion, were Vp and density held fixed? If so, where did the values come from?

Reply: Thank you for your comment. In the OBS receiver function inversions, we used the Vp and density values from the nearby global model CRUST1.0 (Laske et al., 2013) and kept them fixed during the inversions, as receiver functions are not highly sensitive to these parameters. The same Vp values were also applied in the H–κ method to ensure consistency. In addition, the receiver function waveforms from all events at each station were linearly stacked prior to performing the waveform inversion. These clarifications have been added in the revised manuscript at Lines 196–199.

6. In Figure 5, the H results look spatially coherent, but I don't think the k results do. The authors implicitly recognize this by not basing much interpretation on the k results, but it should be clearly stated in the text that a decision was made not to use them (this is not unusual for H-k results from noisy/limited data -- H is more robust).

Reply: We thank the reviewer for pointing this out. Indeed, our Vp/Vs results are consistent with the low-velocity anomalies beneath the corresponding OBS stations. The apparent lack of spatial coherence mainly arises from the presence of thick sedimentary cover, which becomes progressively thicker toward the east. Because sediments are characterized by unusually high Vp/Vs ratios, they strongly affect the overall κ estimates. For example, at station C21F, where the sediment thickness is only about 0.2 km, the obtained κ value is very reasonable and close to the expected value for normal oceanic crust. In contrast, the sedimentary effects are more pronounced at stations located above the oceanic crust (C18F, C12F, C09G, C21F), the accretionary prism (C08F, C28F), and the thinned continental crust in the Makassar Strait (M01F, M02F, M03F). These sedimentary effects may introduce some uncertainties in the absolute κ values, but the relative variations among stations remain robust.

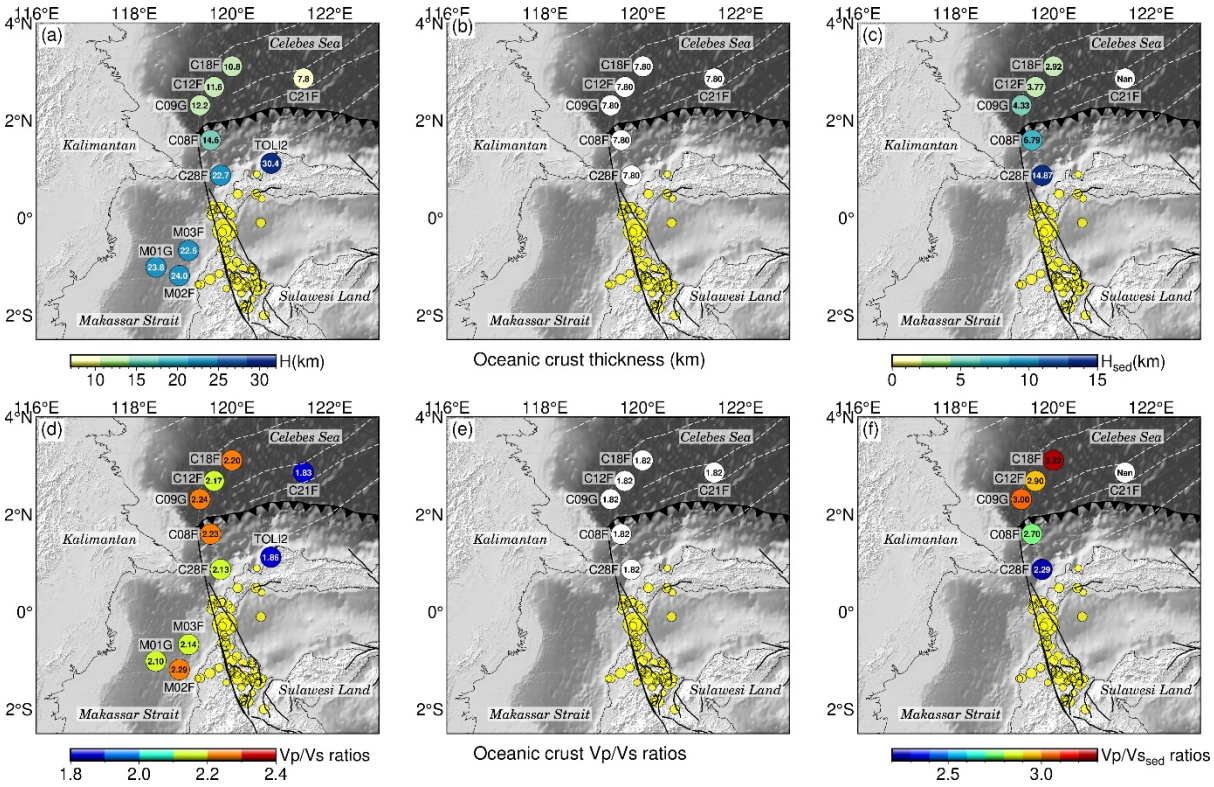

Figure R1: (a) Thickness of the crust above the Moho; (b) Thickness of the oceanic crust; (c) Thickness of the sedimentary layer; (d) Vp/Vs ratios above the Moho; (e) Vp/Vs ratios of the oceanic crust; (f) Vp/Vs ratios of the sedimentary layer. (The black solid line represents the Palu–Koro fault (Patria and Putra, 2020), and the yellow solid circles represent the epicentre distribution of the earthquake after relocation.)

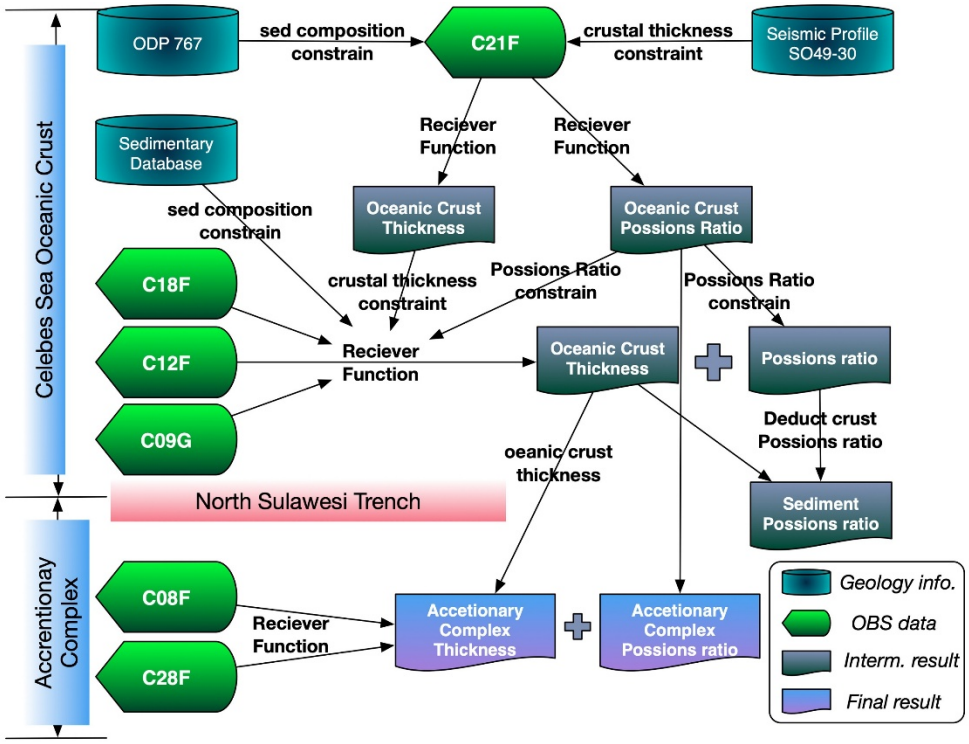

Figure R2: Flowchart of the estimation procedure for sedimentary layer thickness and Vp/Vs ratio.

7. The earthquake relocation work described on page 11 is a new result, so there should be a bit more detail on how it was obtained. What stations were used? Were the OBS data included?

Reply: Thank you for your comment. Since the Palu earthquake occurred in September 2018, while our OBS deployment took place from August 2019 to August 2020, no OBS data were available for this event. Therefore, we used the China Array network data as auxiliary information to assist in the relocation analysis. This result is only used as supporting information to assist in interpreting the tectonic setting, and this has been clarified in the revised manuscript at Lines 266–270.

References

Hable, S., Sigloch, K., Barruol, G., Stähler, S.C., and Hadziioannou, C.: Clock errors in land and ocean bottom seismograms: high-accuracy estimates from multiple-component noise cross-correlations, Geophysical Journal International., 214(3), 2014–2034, doi:10.1093/gji/ggy236, 2018.

Laske, G., Masters., G., Ma, Z. and Pasyanos, M.: Update on CRUST1.0–A 1–degree Global Model of Earth's Crust, Geophys. Res. Abstracts, 15, Abstract EGU2013–2658, 2013.

Ligorria, J.P., and Ammon, C.J.: Iterative deconvolution and receiver-function estimation, Bulletin of the Seismological Society of America., 89, 1395–1400, doi: 10.1785/BSSA0890051395, 1999.

Niu, F., and Li, J.: Component azimuths of the CEArray stations estimated from P-wave particle motion, Earthquake Science., 24, 3–13, doi:10.1007/s11589-011-0764-8, 2011.

Patria, A., and Putra, P.S.: Development of the Palu-Koro Fault in NW Palu Valley, Indonesia, Geoscience Letters., 7, doi:10.1186/s40562-020-0150-2, 2020.

Yang, T.W., Xu, Y., Nan, F.Z., Cao, D.P., Liu, L.H., and Hao, T.Y.: Construction and application of preprocessing technology for passive source ocean bottom seismometer data, Chinese Journal of Geophysics (in Chinese)., 66(2), 746–759, doi: 10.6038/cjg2022Q0076, 2023